Physica Scripta. Vol. T115, 897–900, 2005

XAFS Study on the Trace Amounts of Ytterbium Ions Incorporated in Calcium Carbonate Crystal

H. Tsuno[1*], H. Kagi[2], Y. Takahashi[3], T. Akagi[4] and M. Nomura[5]

[1]Institute for Environmental Management Technology, National Institute of Advanced Industrial Science and Technology (AIST), AIST Tsukuba West, Tsukuba 305-8569, Japan
[2]Graduate School of Science, The University of Tokyo, Tokyo 113-0033, Japan
[3]Graduate School of Science, Hiroshima University, Hiroshima 739-8526, Japan
[4]Faculty of Agriculture, Tokyo University of Agriculture and Technology, Tokyo 183-8509, Japan
[5]Photon Factory, Institute of Materials Structure Science, KEK, Tsukuba 305-0801, Japan

Received June 26, 2003; accepted in revised form November 4, 2003

PACS numbers: 61.10.Ht, 91.65.Nd

Abstract

We measured XAFS spectra of trace amount of ytterbium (Yb) incorporated in calcite, a stable phase of calcium carbonate. Calcium carbonate was precipitated from a mixed solution of $CaCl_2$ aq and $NaHCO_3$ aq with a given amount of $YbCl_3$. Concentrations of Yb were 5 μmol kg^{-1} in the starting solutions and Yb/Ca molar ratio in the precipitated calcium carbonate was 1.2×10^{-3}. Ytterbium L_{III}-edge XAFS spectra were collected in the fluorescence mode at the beamline BL-12C of the KEK-PF. Analysis of the XAFS results indicated, (1) Approximately 15% Yb ion existed as divalent ions in the calcite. (2) Yb^{3+}, major Yb species in the calcite, is located at the Ca^{2+} site in the calcite. The local structure around Yb^{3+} is significantly different from that of Ca^{2+}. The coordination number of Ca^{2+} in the crystal structure of calcite is 6 and Ca-O distance is 2.36 Å. In contrast, the nearest Yb-O coordination for Yb-doped calcite is split into two shells, the nearest 4 oxygen atoms and the second nearest 2 oxygen atoms, and their Yb-O distances are 2.24 Å and 2.77 Å, respectively. It was shown that localized structural relaxation occurred around Yb^{3+} which has smaller ionic radius than Ca^{2+}.

1. Introduction

Exploring the detailed chemical mechanism of dissolution and crystallization of calcium carbonate ($CaCO_3$) is one of the crucial issues in understanding the global cycling of CO_2 on the earth surface. Trace amount of rare earth elements (REEs) induces significant effects on the crystal growth and dissolution of calcium carbonate [1–4]. The substantial increase in the solubility of $CaCO_3$ [1, 2], the stabilization of the vaterite (labile phase of $CaCO_3$) [2, 4] and the inhibition of calcite growth [3] were caused by the addition of trace amount of lanthanum into the aqueous system. Furthermore, enrichment of REEs in calcium carbonate was shown by several studies [5, 6]. Very little is known about the uptake mechanism of REEs in calcium carbonate and their chemical state. X-ray absorption fine structure (XAFS) is practically the only method for the structural characterization of trace elements in solid materials [7]. XAFS in a fluorescence mode offers the advantage of element-discrimination and potentially high sensitivity to trace elements. In the present work, we investigated the chemical species of ytterbium incorporated in calcite and the local structure around it using X-ray absorption near-edge structure (XANES) and Extended X-ray absorption fine structure (EXAFS) techniques.

2. Experimental procedure

2.1. *Precipitation procedure*

Yb-doped calcium carbonate was prepared from a mixture of calcium chloride and sodium hydrogen carbonate solutions (30 mmol kg^{-1}, respectively) containing a given amount (5 μmol kg^{-1}) of ytterbium chloride. The experiments were conducted in a closed system in a surface-silanized glass vessel at 30°C. The starting solution was transferred into the vessel and immediately sealed with a silicone rubber stopper in which a pH electrode was embedded [2]. The amount of precipitate and ion activity products (IAP = $\gamma\ Ca^{2+}\ [Ca^{2+}] \times \gamma CO_3^{2-}\ [CO_3^{2-}]$) were calculated from the initial concentrations of all the chemical species in the system and pH at each sampling time after a previously reported method [1, 2]. The pH of solution changed from 7.8 at the beginning of reaction to 6.4 at the end of reaction. After standing for 1 day, the precipitate was filtered with a membrane filter with a pore size of 0.45 μm (Millipore® HAWP 024 00), rinsed with milli-Q water and dried at 110°C. Powder X-ray diffraction pattern indicated that the sample obtained was composed of calcite exclusively. The concentrations of Yb in the precipitates were determined by an inductively coupled plasma atomic emission spectrometer (ICPS-7000, Shimadzu Inc.). The concentrations of Yb in the synthesized calcite samples were about 1.1×10^{-3} in Yb/Ca molar ratio. $Yb(OH)_3$, $NaYb(CO_3)_2 \cdot n(H_2O)$, Yb_2O_3, $Yb_2(CO_3)_3 \cdot n(H_2O)$ powders and 5 mmol kg^{-1} $YbCl_3$ solution were used as standard materials of XANES measurements.

2.2. *XAFS spectroscopy*

XAFS spectra were collected in the fluorescence mode at the beamline BL-12C of the Photon Factory, High Energy Accelerator Research Organization (KEK-PF) in Tsukuba, Japan [8]. The KEK-PF storage ring was operated at 2.5 GeV with a maximum current of 450 mA. An Si(111) double-crystal monochromator was used to produce a monochromatic X-ray beam, with one crystal detuned for reduction of harmonics and the beam was focused into an area smaller than 1 square mm by a bent cylindrical mirror [8]. The Yb L_{III} (8947 eV) absorptions of samples were measured by the fluorescence yield (Yb Lα: 7.4 keV) using a 19 elements pure Ge solid-state detector with energy resolution sufficient to separate Yb signals from elastic scattering and fluorescence of other elements [9, 10]. The energy region around Yb-Lα fluorescence was selected by single-channel analyzers

*e-mail: h.tsuno@aist.go.jp

(SCA). The monochromator was calibrated at 8947 eV (Yb L_{III} absorption edge) using ytterbium oxide powder. XAFS spectra of solid samples were measured at approximately 20 K. The incident X-ray intensity (I_0) was monitored by an ion chamber which was filled with nitrogen gas. The X-ray absorption (μ) is expressed as $\mu = I_f/I_0$, where I_f is the intensity of fluorescence X-ray and μ is plotted against incident X-ray energy. Multiple scans (typically 3–5 times) were carried out for each sample and then averaged. The averaged XAFS spectra were converted to k space. The atomic contribution to the absorption coefficient (μ_0) was regarded as the smooth background in the EXAFS region of the each averaged XAFS spectra by a cubic spline method. $\chi(k)$ was extracted as usual and Fourier transformed into r-space. Determination of average interatomic distance, coordination number, and Debye-Waller factor for the isolated shell about an absorber in an unknown material were made by least-square fitting of the Fourier-filtered $\chi(k)$ function. Analyses of the EXAFS spectra were performed with the PC program, REX2000 (Rigaku Co.), which uses theoretical phase functions and amplitudes from McKale's table [11]. The interatomic distances and coordination numbers were given by fitting with errors of respectively ±0.02 Å and ±15–20%, assuming that systematic errors have been minimized in the experiment and data analysis. XANES spectra were also deconvoluted by REX2000 (Rigaku Co.).

3. Results and discussion

3.1. *XANES: Spontaneously induced reduction of trivalent ytterbium in calcite*

XANES spectra of the calcite and Yb-bearing standard materials had a significant white line around 8948 eV, which was assigned to electron transition 2p→5d6s of Yb^{3+} [12, 13]. The XANES spectrum of Yb in calcite is shown in Fig. 1. A discernible shoulder (A) is observed in the lower energy side of the main white line (B). This shoulder was not observed on XANES spectra of Yb-bearing materials. We attempted to fit the main peak at 8948 eV and the shoulder by a couple of a Gaussian function for white line and an arctangent function for continuum absorption, respectively. The deconvoluted components of XANES spectrum of Yb in calcite are shown in Fig. 1. A small peak (A) was resolved from the spectrum of calcite. Resultant peak position, peak height and FWHM of Gaussian curve for Peak A are 8940.2 eV, 0.14 a.u. (arbitrary unit) and 6.1 eV, and those for Peak B are 8948.6 eV, 0.88 a.u. and 6.1 eV, respectively. The position of Peak A was at lower energy by 8 eV than that of Peak B and is close to that of the absorption of Yb^{2+} [12–15]. Thus, we attributed peak A to Yb^{2+}. These results indicate that significant proportion of ytterbium existed as divalent ions in the calcite structure. Tanaka *et al.* suggested that the ratio of areas of peak A and B indicates directly the relative amounts of Yb^{2+} and Yb^{3+} [13]. Based on the report, we calculated that the 14–17% of Yb exists as Yb^{2+} in calcite. Thermodynamic calculation indicates that the $[Yb^{2+}]/[Yb^{3+}]$ ratio in the starting solution is smaller than 10^{-31}. In the starting solutions, trivalent ytterbium was predominant and divalent ion was negligible. This suggests that a part of Yb was reduced at some stage of calcium carbonate formation.

Yb^{3+} substitutes in the six-fold coordination for the Ca^{2+} site in calcite as mentioned in the following section. The ionic radii of Ca^{2+}, Yb^{3+} and Yb^{2+} in the six-fold coordination are 1.00, 0.868 and 1.02 Å, respectively [16]. The ionic radius of Yb^{2+} is quite close to that of Ca^{2+}. It is expected that Yb^{2+} can substitute at the calcium site of calcite with higher stability (affinity) than Yb^{3+} without significant mismatches in ionic radius as well as the ionic valence. For the stabilization of Yb^{2+} in the calcite structure, it is possible that some defects such as oxygen vacancy in the crystal structure of calcite can compensate the formation of Yb^{2+} in the oxidative condition. Further information of this result is described in Tsuno *et al.* 2003 [17].

3.2. *EXAFS: The local structure of Yb^{3+} incorporated in calcite*

The extended X-ray absorption fine structure (EXAFS) spectra of Yb in calcite can be attributed to Yb^{3+}, the major species in calcite, although we showed the presence of Yb^{2+} in calcite on the previous section. We regarded the structural information of Yb for EXAFS analysis as Yb^{3+}. The k^3-weighted $\chi(k)$ EXAFS of Yb incorporated in calcite is shown in Fig. 2. The spectrum collected at 20 K showed better S/N ratio than that taken at Room temperature, thus, it was used for detailed analysis. We adopted the spectrum at 20 K for the EXAFS analysis. Fig. 3

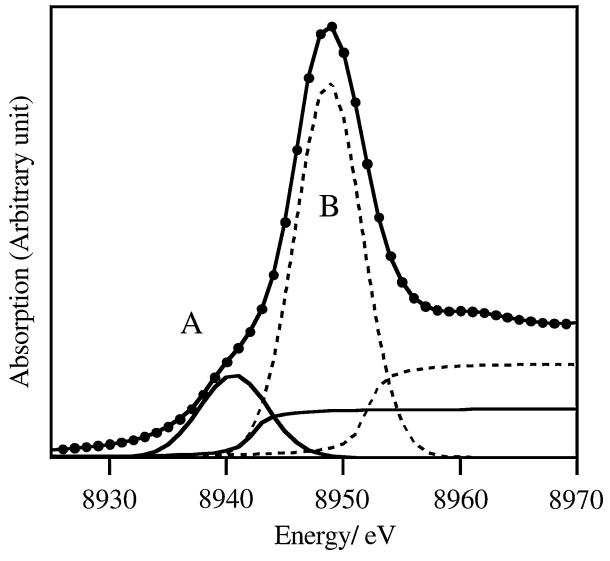

Fig. 1. Yb L_{III} edge normalized XANES and the deconvoluted spectra of Yb incorporated in calcite. A: Yb^{2+}, B: Yb^{3+}.

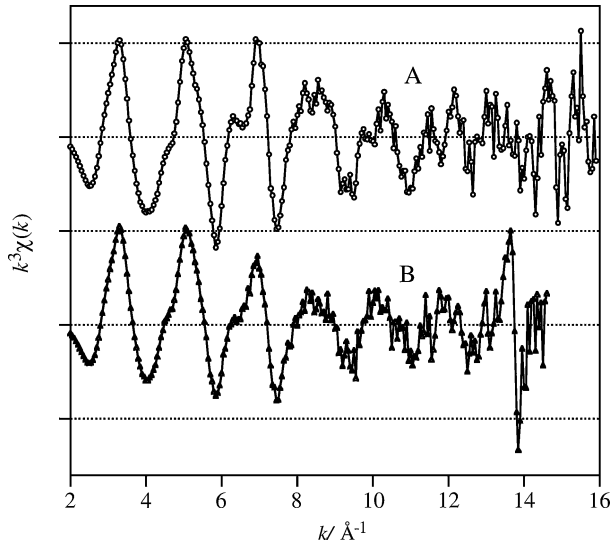

Fig. 2. The k^3-weighted $\chi(k)$ spectra for Yb incorporated in calcite. A: collected at 20 K, B: at room temperature.

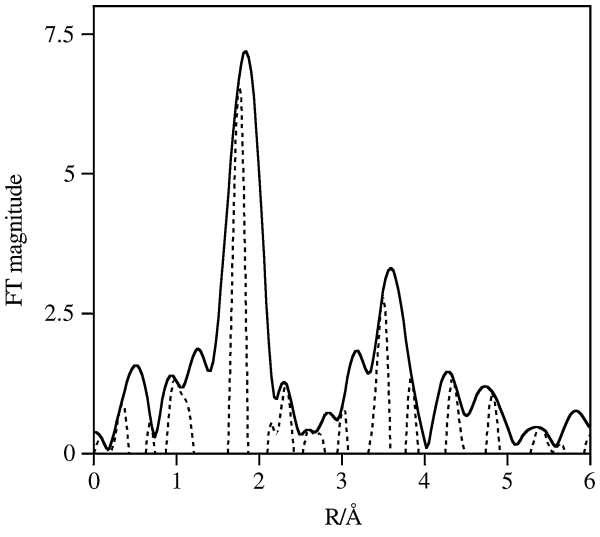

Fig. 3. Fourier transform of k^3-weighted Yb L_{III} EXAFS of Yb in $CaCO_3$ (no phase shift correction). Solid line: Radial structure function; Dashed line: imaginary part of FT.

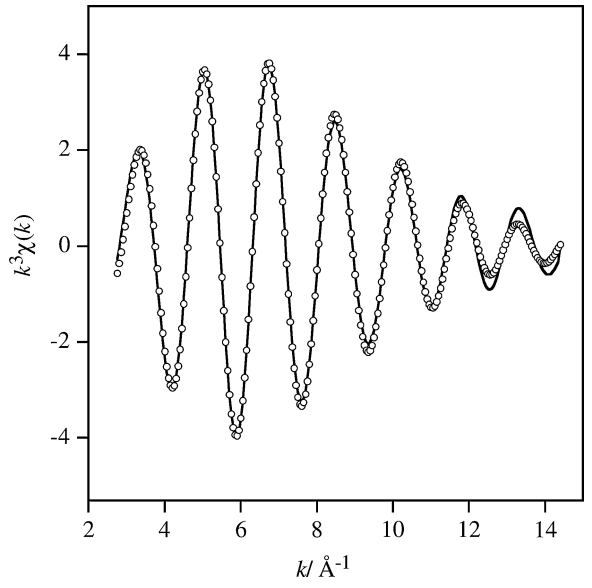

Fig. 4. Fit to the back Fourier transform of the first peak of k^3-weighted Yb L_{III} FT-EXAFS data shown in Fig. 3 performed in the range 1.5–2.1 Å. Open circle: experimental; Solid line: fitting.

shows Fourier transform of k^3-weighted $\chi(k)$ EXAFS of Yb-doped calcite (without phase-shift correction). A peak of radial structure function at about 1.8 Å is attributed to the nearest Yb-O interaction by assuming that Yb^{3+} occupies the Ca^{2+} site in calcite. The rough fitting for the back Fourier transform of the first peak in Fig. 3 brought the coordination number (N) as 4 and the larger residue of the fitting. It is an unreasonable value for Yb^{3+} coordination in calcite structure. Thus, we assumed that the first O-shell for Yb in calcite was splitting to near two shells. Fig. 4 shows the back Fourier transform of the first peak of k^3-weighted Yb L_{III} FT data between 1.5–2.1 Å shown in Fig. 3. The best fitting result indicates that there are 4 O atoms at 2.24 Å and 2 O atoms at 2.77 Å. The nearest Yb-O distance (2.24 Å) is comparative to the calculated Yb-O distance from the sixfold ionic radii of Yb^{3+} from Shanonn 1976 [16]. The nearest Yb-O distance (2.24 Å) in calcite is smaller than Ca-O distance (2.360 Å) of pure calcite [18]. Although the coordination number of Ca^{2+} for calcite is 6, all the

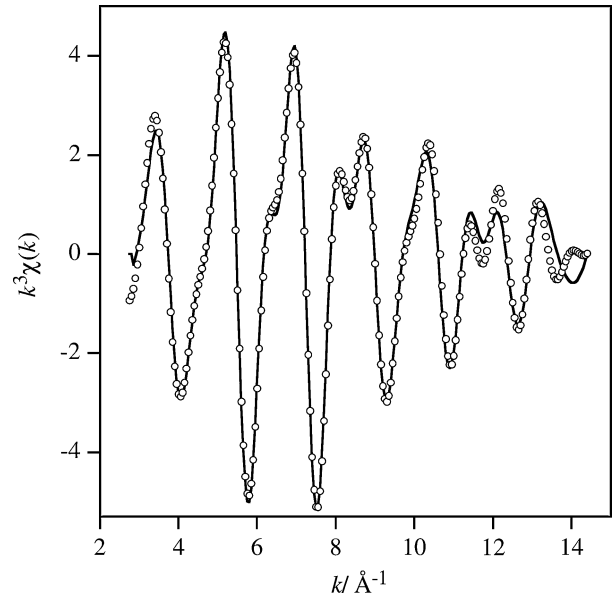

Fig. 5. The k^3-weighted Yb L_{III} edge EXAFS data, $\chi(k)$, for the calcite sample and the best-fit multishell model as a function of wave vector k. The data were fit with parameters described Table I. Open circle: experimental; Solid line: fitting.

six oxygen atoms could not be located in the same nearest shell to occupy Yb^{3+} at Ca^{2+} site in calcite. Thus, 4 oxygen atoms are located at the nearest shell with an Yb-O distance of 2.24 Å, while 2 oxygen atoms are pushed away from the nearest shell to a little far position. It was shown that the localized structural relaxation occurred around Yb^{3+} which has smaller ionic radius than Ca^{2+}.

Elzinga *et al*. showed that the nearest Yb-O shell in their Yb-doped calcite samples has coordination number of 7.5 and Yb-O distance 2.24 Å by EXAFS analysis [19]. Their fitting results had reasonable Yb-O distance but considerably large coordination number at Ca site in calcite structure. Thus, they fixed coordination number of 6 as chemical reasonable number from a comparison of the observed Yb-O distance with values predicted from sixfold and sevenfold ionic radii from Shanonn [16]. In contrast, our results are derived directly from EXAFS analysis and the distortion of YbO_6 octahedron was detected from the analysis.

For the Ca site of the calcite structure, the shells have the six nearest oxygen atoms at 2.360 Å, the nearest carbon atoms at 3.213 Å, the second nearest oxygen atoms at 3.459 Å, and calcium atoms at 4.048 Å and they have ideal coordination numbers (N) of 6 [18]. The mean Yb-O distance in calcite was 2.42 Å from the present experimental results. This mean value of Yb-O distance agrees with the size of the Ca^{2+} site in calcite. According to calcite structure, the coordination numbers of shells beyond the first oxygen group were fixed as 6 during refinement to reduce the

Table I. *Multishell best-fit parameters for Yb L_{III} EXAFS incorporated in calcite. N: coordination number; R: radial distance; σ: Debye-Waller factor.*

Shell	N	R(Å)	σ(Å)
Yb-O	4.1	2.24	0.066
Yb-O	1.9	2.77	0.119
Yb-C	6*	3.25	0.064
Yb-O	6*	3.34	0.110
Yb-Ca	6*	4.04	0.088

*Parameter fixed during refinement to reduce the number of fit parameters.

number of fit parameter. The k^3-weighted Yb L_{III} edge EXAFS data, $\chi(k)$, for the calcite sample and the best-fit multishell model were shown in Fig. 5. The results were well fit with the observation values. Best-fit parameters for Yb^{3+} incorporated in calcite are shown in Table I. The EXAFS fitting results support that Yb occupied the Ca sites in calcite as was expected.

Acknowledgement

The XAFS experiments were performed under the approval of the Photon Factory Program Advisory Committee (99G075 and 2001G122). This research was supported by Nissan Science Foundation and by a Grant-in-Aid (11304040, 13554018) from the Ministry of Education, Science, Sports and Culture. This study has been financially supported in part by the Research Fellowships of the Japan Society for the Promotion of Science for Young Scientists to H. T.

References

1. Akagi, T. and Kono, Y., Aquat. Geochem. **1**, 231 (1995).
2. Tsuno, H., Kagi, H. and Akagi, T., Bull. Chem. Soc. Jpn. **74**, 479 (2001).
3. Kamiya, N., Kagi, H., Notsu, K., Tsuno, H. and Akagi, T., Chem. Lett. **2002**, 890 (2002).
4. Tsuno, H., Kagi, H. and Akagi, T., Chem. Lett. **2002**, 960 (2002).
5. Terakado, Y. and Masuda, A., Chem. Geol. **69**, 103 (1988).
6. Zhong, S. and Mucci, A., Geochim. Cosmochim. Acta **59**, 443 (1995).
7. Brown Jr., G. E., Calas, G., Waychunas, G. A. and Patiau, J., "Reviews in mineralogy, Volume 18: Spectroscopic methods in mineralogy and geology". (edited by Hawthorne, F. C.) (Mineralogical Society of America, 1988), p. 431.
8. Nomura, M. and Koyama, A., KEK Report **95–15**, 1 (1996).
9. Nomura, M., KEK Report **98–4**, 1 (1998).
10. Nomura, M., J. of Synchrotron Radiat. **5**, 851 (1998).
11. Mckale, A. G., Veal, B. W., Paulikas, A. P., Chan, S. K. and Knapp, G. S., J. Am. Chem, Soc. **110**, 3763 (1988).
12. Hatwar, T. K. *et al*., Solid State Commun. **34**, 617 (1980).
13. Tanaka, T., Hanada, T., Yoshida, S., Baba, T. and Ono, Y., Jpn. J. Appl. Phys. **32**, 481 (1993).
14. Rao, C. N. R. *et al*., Chem. Phys. Lett. **76**, 413 (1980).
15. Baba, T. *et al*., J. Chem. Soc., Faraday Trans. **89**, 3177 (1993).
16. Shannon, R. D., Acta Crystallogr. **A32**, 751 (1976).
17. Tsuno, H., Kagi, H., Takahashi, Y., Akagi, T. and Nomura, M., Chem. Lett. **32**, 500 (2003).
18. Effenberger, H., Mereiter, K. and Zemann, J., Z. Kristallogr. **156**, 233 (1981).
19. Elzinga, E. J. *et al*., Geochim. Cosmochim. Acta **66**, 2875 (2002).